

TeraHertz Antiresonance Phononic Mirrors with Tunable Frequency based on Atomic-Scale Metamaterials

Haoxue Han,^{1,*} Lyudmila G. Potyomina,² Alexandre A. Darinskii,³ Sebastian Volz,^{1,†} and Yuriy A. Kosevich^{1,4,‡}

¹*Laboratoire d'Énergetique, Moléculaire, Macroscopique et Combustion, CNRS UPR 288, Ecole Centrale Paris, Châtenay-Malabry 92295, France*

²*Department of Physics and Technology, National Technical University "Kharkiv Polytechnic Institute", Frunze ul. 21, Kharkov 61002, Ukraine*

³*Institute of Crystallography, Russian Academy of Sciences, Leninskii pr. 59, Moscow 119333, Russia*

⁴*Semenov Institute of Chemical Physics, Russian Academy of Sciences, Kosygin str. 4, Moscow 119991, Russia*

(Dated: February 19, 2014)

We introduce and model an atomic-scale phononic metamaterial producing interference antiresonances for sound waves and controlling the heat flux spectrum. We show that a crystal plane partially embedded with defect-atom arrays generates a total phonon reflection at the frequency prescribed by masses and interaction forces. The random distribution of the defects in the plane and the anharmonicity of atom bonds do not deteriorate the antiresonance. Such patterned atomic planes can be considered as high-finesse atomic-scale phononic mirrors which can be tuned by the adjustment of the vibrational properties of the defect atoms and selective patterning of the defect-atom arrays. All our conclusions are confirmed both by analytical studies of the equivalent one-dimensional lattice models and by numerical molecular dynamics simulations of realistic three-dimensional lattices.

Resonance coupling between continuum and embedded discrete states can result in asymmetric non-Lorentzian resonance absorption, which was first described by Fano[1] in his study of inelastic autoionization resonance in atoms. Resonances with Fano-like asymmetric profiles have been observed in various nanostructures, such as plasmonic structures[2–4], photonic crystals[5, 6] and metamaterials[7, 8]. In particular, the enhanced electromagnetic (EM) reflection induced by Fano-like resonances, achieved in metafilms embedded with splitting arrays[7] and in stereometamaterials[9], has offered the prospect of a multitude of applications as quantum optics[10] and negative refraction[11]. For the sound waves, the enhanced phonon reflection was first described in Ref.[12] and Ref.[13] independently. In Ref.[12], the anomalous reflection and absorption of acoustic waves in a crystal with two-dimensional (2D) defect was interpreted as *destructive interference* between two phonon paths: through the nearest-neighbor bonds and through the non-nearest-neighbor bonds which couple directly atomic layers adjacent to the defect plane. In Ref.[13], an analogy between electron and phonon scattering was drawn and phonon transmission with Fano-like asymmetric profile through a strip of oscillator chains connected in parallel was calculated numerically.

In this Letter we introduce and model an atomic-scale phononic metamaterial that allows to manipulate the flow of thermal energy based on phonon interference antiresonances by exploiting the phonon reflection on internal interfaces embedded with defect-atom arrays. The key idea is to introduce planar defects that force phonons to propagate through two paths: through unperturbed (matrix) and perturbed (defect) interatomic bonds [12, 14]. The resulting wave interference results

in transmission antiresonances (reflection resonances) in the spectrum of thermal phonons that can be controlled by the masses, force constants and distribution of the defect atoms. Our results show that the patterning of the defect-atom arrays can lead to a new departure in thermal energy management, offering potential applications in heat imaging[15, 16], thermo-optics[17, 18] and thermal cloaking[19].

Phonon antiresonances caused by the interference between phonon channels can be understood with the use of an equivalent model of monatomic one-dimensional (1D) lattice of coupled harmonic oscillators[14], depicted in the inset in Fig. 1. In model (a), phonons propagate through two paths: (i) through the host atom bonds, and (ii) through those of the impurity atoms, whereas in model (b), only the second channel remains open. Under the assumption of small amplitude waves, the atomic displacements can be written in the plane-wave form $u_n = u_0 e^{i(\omega t - kn)}$, where the integer n marks the lattice site number in the chain, ω and k are the frequency and wave number. The equivalent 1D lattice model gives the following energy transmission coefficient α , see also [12]:

$$\alpha(\omega) = \frac{(\omega^2 - \omega_R^2)^2 (\omega_{\max}^2 - \omega^2)}{(\omega^2 - \omega_R^2)^2 (\omega_{\max}^2 - \omega^2) + C\omega^2 (\omega^2 - \omega_T^2)^2}, \quad (1)$$

where $\omega_{R,T}$ are the frequencies of the reflection and transmission resonances, ω_{\max} is the maximal phonon frequency for a given polarization in the chain and $\omega_R < \omega_T < \omega_{\max}$. C is a real positive coefficient given by the atomic masses and force constants. The ω_R frequency exists only in the presence of an additional channel which is open for wave propagation through the bypath around the defect atom, see inset in Fig. 1. The total reflections ($\alpha = 0$) arise at the resonant reflection frequency

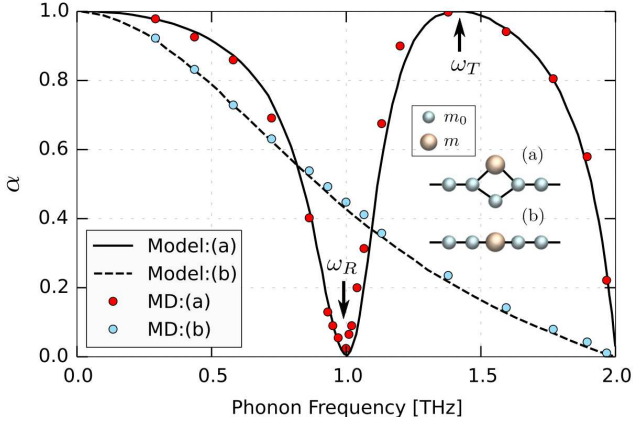


FIG. 1. (color online). Spectra of phonon transmission coefficient α predicted by equivalent model of monoatomic 1D lattice and by MD simulations of a 3D Ar lattice with planar defect containing heavy impurities, with mass $m > m_0$. (Inset) Two possible 1D lattice models describing phonon propagation through lattice region containing the local defect: (a) phonons can propagate through defect and host atoms bonds; (b) phonons can propagate only through defect atom bonds. The solid and dashed lines describe the plane-wave solutions from the analytical calculations for lattice model (a) and (b), respectively. The colored circles are MD simulation results. The analytical calculations and MD simulations were performed for $m = 3m_0$.

$\omega = \omega_R$ and at maximal frequency $\omega = \omega_{\max}$, while the total transmissions ($\alpha = 1$) appear at zero frequency $\omega = 0$ and at resonant transmission frequency $\omega = \omega_T$. In a lattice with atomic impurities, the substituent atoms scatter phonons due to differences in mass and/or bond stiffness. Since no bond defect was introduced, the loci of the resonances are only determined by the mass of the isotope atoms. The analytical 1D lattice model gives the following expression for resonance-reflection frequency:

$$\omega_R = \frac{\omega_{\max}}{\sqrt{m/m_0 + 1}}, \quad (2)$$

where m and m_0 refer to the atomic mass of the defect and host atom, $m > m_0$. Eq. (2) reveals that the reflection resonance experiences the isotopic shift. The transmission resonance at $\omega = \omega_T$ is much less sensitive to the defect mass since it is largely determined by the mass of the host atom. In the spectrum of the transmission coefficient α , as depicted in Fig. 1, strong reflection resonance at ω_R is followed by an enhanced transmission at ω_T in the model (a), whereas both the resonance minimum and maximum are completely suppressed and replaced by a monotonous decay of transmission with frequency in model (b). This effect provides a clear evidence for the influence of the additional channel on the propagation and scattering of phonons in a multichannel system [14]. This behavior is reminiscent of the Fano resonances produced by the coupling of a discrete state to a continuum[1],

which have also been observed in experiments on light scattering by hole arrays in metallic films[20]. The low transmission at short wavelength near the Brillouin zone edge can be attributed to the low phonon group velocity. It is worth mentioning that model (b) can also provide resonance total phonon transmission through the lattice plane embedded with defect atoms, weakly coupled with the matrix, but the 100% filling by the defect atoms does not provide resonance reflection because of the absence of the second phonon path through such plane[12, 21].

This phonon antiresonance is confirmed to persist in a realistic three-dimensional (3D) lattice, modeled with the use of Molecular Dynamics (MD) simulations[22]. An atomic-scale phononic metamaterial is achieved by embedding a two-dimensional (2D) array of heavy defect atoms segregated by the host atoms in a crystal plane of a 3D lattice. The impurity-atom arrays can be distributed periodically or randomly in the defect crystal plane with different filling fractions. When the impurities do not fill entirely the defect plane, phonons have two paths to traverse such an atom array in analogy with the 1D model (a) in Fig. 1, whereas the phonon path through the host atoms is blocked when the defect layer is constituted by a uniform impurity-atom array, as described by model (b) in Fig. 1. Two types of atomic-scale metamaterials were studied: (i) a monoatomic lattice of Argon (Ar) where the impurities are heavy isotopes of Ar and (ii) a diamond lattice of Si with Germanium (Ge) atoms as the impurities. The interactions between Ar atoms are described by the Lennard-Jones (LJ) potential. The covalent Si:Si/Ge:Ge/Si:Ge interactions are modeled by the Stillinger-Weber (SW) interatomic potential[23].

For the purpose of probing the phonon transmission across the defect-atom arrays, MD-based phonon wave-packet method[24] was used to provide a per-mode transmission coefficient and highlight the spectrum structure versus the defect masses. A wave packet centered at the wave vector \mathbf{k} in the reciprocal space and at \mathbf{r}_0 in the real space is generated by assigning the displacement \mathbf{u}_i for the atom i as:

$$A\epsilon(\mathbf{k}) \exp[i(\mathbf{k} \cdot (\mathbf{r}_i - \mathbf{r}_0) - \omega t)] \exp(-|\mathbf{r}_i - \mathbf{r}_0|^2/\xi^2)$$

where A is the wave amplitude, $\epsilon(\mathbf{k})$ the phonon polarization vector, ξ the spacial extent of the wave packet, and ω the eigenfrequency for \mathbf{k} in a single branch of the phonon dispersion curve. Unless otherwise specified, the wave amplitude A of the incident phonons is considered sufficiently low such that anharmonic coupling to other lattice modes is so weak that the wave packets propagate in effectively harmonic crystal without any perceptible spreading or scattering. The wave packet was set to propagate normally to the defect layer where elastic scattering results in transmitted and reflected waves. Phonon transmission coefficient $\alpha(\omega, \mathbf{k})$ is defined as the ratio between the energy carried by the transmitted and the initial wave packet for a given phonon mode (ω, \mathbf{k}) [24].

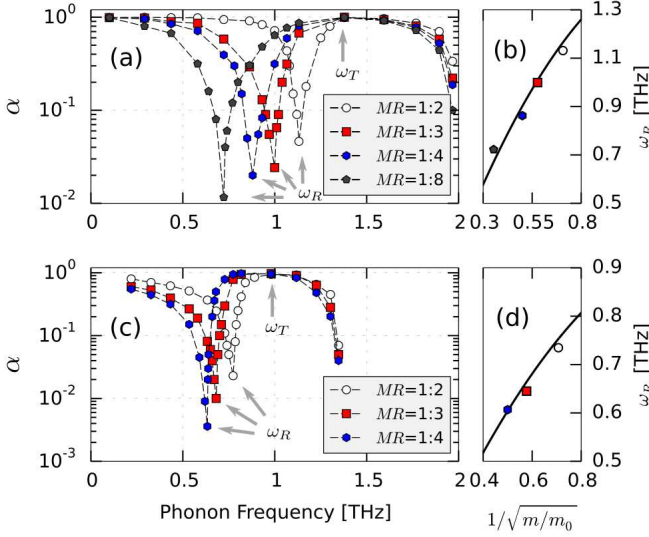


FIG. 2. (color online). Spectra of phonon transmission coefficient α for (a) LA and (c) TA mode in the phononic metamaterial, which consists of 2D array of periodically alternating isotopes of different masses with a filling fraction of 50% in a 3D Ar lattice. The mass ratio (MR) is the ratio between the mass of the host atom m_0 and that of the isotope m . Isotopic shift of the reflection resonances versus the mass ratio for (b) LA and (d) TA modes. The symbols present the resonances from MD simulations and the solid curves define the analytical prediction of the 1D lattice model calculations.

The transmission coefficient α , retrieved from MD simulations of an Ar metamaterial with 2D periodic defect-atom array, demonstrates an excellent agreement with the plane-wave solutions of the equivalent 1D lattice model, presented together in Fig. 1. The incident phonons undergo strong reflection at the defect layer at $\omega = \omega_R$ for both longitudinal acoustic (LA) and transverse acoustic (TA) modes, Fig. 2(a) and (c), which is followed by phonon transparency with total transmission at $\omega = \omega_T$. Phonon transmission spectra display the interference antiresonance profiles since both the destructive, at $\omega = \omega_R$, and constructive, at $\omega = \omega_T$, interferences occur due to the presence of the two phonon pathways.

As the defect atoms get heavier, the destructive resonance becomes more pronounced in terms of phonon reflection depth and width, and demonstrates a red-shift in the phonon transmission spectrum thus impeding the long-wavelength phonons. As depicted in Fig. 2(b) and (d), the spectral positions of the reflection resonances ω_R undergo the isotopic shift, which is again in good agreement with the analytical prediction of the equivalent 1D lattice model given by Eq. (2). We note that a superlattice structure of defect layers in the matrix can further enhance the scattering of thermal phonons since multiple antiresonances in the phonon transmission spectrum will result in a phonon stop band centered at $\omega = \omega_R$ [14].

In Fig. 3(a), the transmission spectra for both longitu-

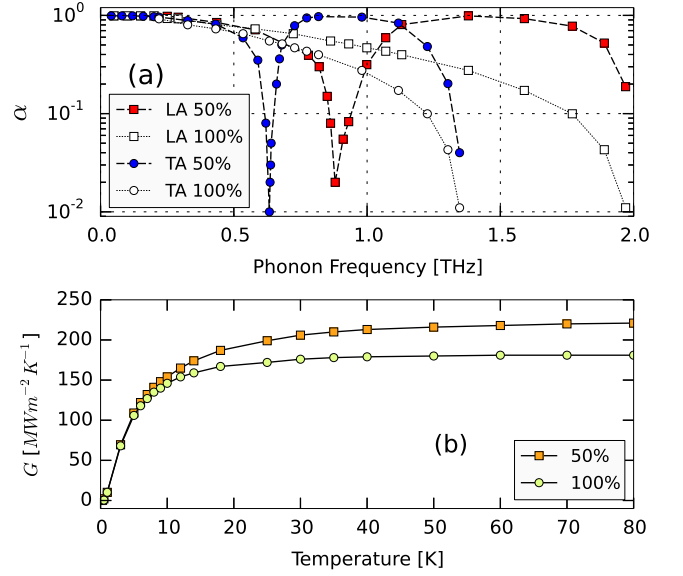


FIG. 3. (color online). (a) Spectra of phonon transmission coefficient α for LA (solid rectangles) and TA (solid circles) phonons through a 50%-filled defect layer and for LA (open rectangles) and TA (open circles) phonons through a uniform defect layer for the defect MR=1:4 in a 3D Ar lattice. The temperature-dependent interfacial thermal conductance across a defect plane 50%-filled with periodic array of impurities (rectangles) and across a uniform defect plane (circles).

dinal and transverse phonons across the defect-atom array, 100% packed with impurity atoms (hereafter referred to as “uniform defect array”), is plotted to be compared with that of the 50%-filled defect-atom array. At the reflection resonance frequency ω_R , a periodic array of alternating defect atoms has a transmittance two orders of magnitude smaller than that of the uniform defect-atom array. The difference between the very strong phonon reflection on a 50%-filled defect array and the high phonon transmission across a uniform defect array can result in a counter-intuitive effect: a defect array with segregated impurity atoms can scatter more thermal phonons than an array with a uniform distribution of heavy isotopes. We calculate the interfacial thermal conductance G by following the Landauer-like formalism[26]:

$$G = \int \sum_{\nu} \hbar \omega(\mathbf{k}, \nu) v_{g,z}(\mathbf{k}, \nu) \alpha \frac{\partial}{\partial T} n_{\text{BE}}(\omega, T) \frac{d\mathbf{k}}{(2\pi)^3}, \quad (3)$$

where \hbar is the reduced Planck constant, $v_{g,z}$ the phonon group velocity in the cross-plane direction, $n_{\text{BE}}(\omega, T)$ is the Bose-Einstein phonon distribution at temperature T , $n_{\text{BE}}(\omega, T) = [\exp(\hbar\omega/k_B T) - 1]^{-1}$, where k_B is the Boltzmann constant. The integral is carried out over the whole Brillouin zone and the sum is over the phonon branches. The thermal conductance as a function of temperature, as is depicted in Fig. 3(b), suggests that although a periodic array of alternating defect atoms is more effective

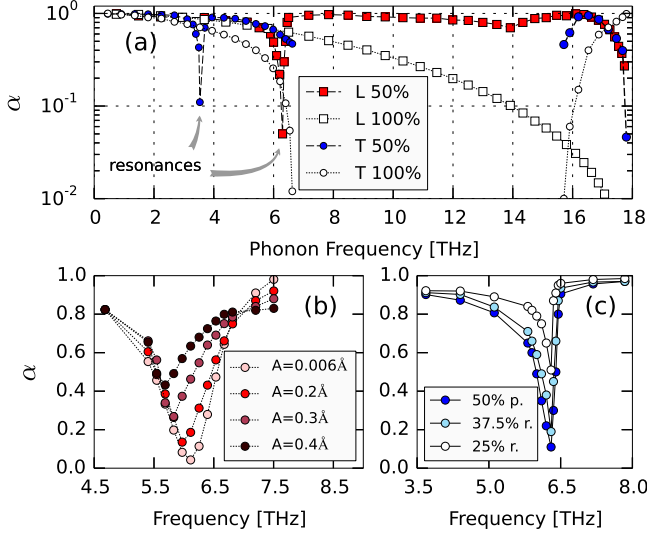


FIG. 4. (color online). (a) Transmission spectra for both longitudinal (LA and LO) and transverse (TA and TO) phonons in a Si phononic metamaterial through the uniform Ge-defect layer (open squares and circles) and through the 50%-filled Ge-defect layer (red squares and blue circles). (b) Evolution of the reflection resonance versus the increasing wave amplitude A . (c) Phonon transmission coefficient α for a defect layer containing randomly dispersed Ge atoms with 37.5% and 25% filling fraction, compared with that of a defect layer containing 50% of periodically alternating Ge atoms.

in blocking thermal phonons than a uniform defect-atom array at the resonance frequency $\omega = \omega_R$, the overall thermal conductance is higher for the partial defect-atom filling due to a higher transmittance of high-frequency phonons with a larger phase space, cf. Eq. (3).

The anomalous phonon transmission phenomenon in molecular systems can find its acoustic counterpart in macroscopic structures[14, 25, 27]. In Ref.[25], perforated plates were proved to shield ultrasonic acoustic waves in water much more effectively than uniform plates. Liu *et al.*[27] managed to break the mass-density law for sonic transmission by embedding high-density spheres coated with a soft material in a single layer of hard matrix.

In Fig. 4, we report the Fano-like interference antiresonance in Si crystal as the metamaterial incorporating 2D planar impurity array of Ge atoms. The mass ratio between Ge and Si atoms is 2.57 and thus the Ge-atom array introduces both heavy mass and bond defects due to a weaker Ge:Si interaction than the Si:Si interaction[23]. Transmission spectra for both longitudinal acoustic (LA) and optical (LO) and transverse acoustic (TA) and optical (TO) phonons across the uniform defect layer are plotted in Fig. 4(a) along with that across the 50%-filled defect array. The long-wavelength phonons from acoustic branches experience strong resonant reflections at the 50%-filled Ge defect array, while the short-wavelength phonons near the edge of the Brillouin zone are strongly

reflected by the uniform defect array.

The nonlinear effects on the phonon Fano resonance were investigated by increasing the amplitude A of the incident phonon wave packet. The evolution of the resonance frequency versus the wave amplitude is shown in Fig. 4(b). As A increases, the reflection becomes less pronounced with more heat flux passing through, which provides direct evidence of inelastic phonon scattering at the defect plane. The resonances demonstrate the red frequency shift due to the higher-order (cubic) terms in the interatomic potential. We note in this connection that our computation of the equivalent 1D atomic chain, containing an impurity atom characterized by non-parabolic (nonlinear) interaction potential with neighboring host atoms, agree with our MD results. The resonance transmission minimum remains pronounced even when the interaction nonlinearity becomes fairly strong. Therefore the phonon antiresonances make it possible to control thermal energy transport in the case of large-amplitude atom oscillations, for instance at very high temperatures.

In contrast to light[28], even a single defect atom in a lattice plane produces transmission antiresonance for phonons. Therefore, phonon reflection should be apparent even for defect-atom arrays in the absence of periodicity because of the localized nature of the resonance. This is supported by further investigation of the phonon transmission through the arrays of Ge atoms, distributed in a crystal plane in Si phononic metamaterial with 37.5% and 25% filling fractions. The measured transmission coefficients, Fig. 4(c), for 37.5% and 25% defect arrays were averaged over different random distributions. Strong transmission dips and frequency regions of enhanced transmission do occur in both cases like in periodic arrays. The resonances remain at the same spectral locations, though the decreased defect density weakens the resonance reflection and narrows the resonance width because the periodicity of ordered arrays facilitates cooperative effects in the transmission through the defect plane. This was proven to be equally valid in macroscopic acoustic metamaterials[27].

In conclusion, we introduce and provide comprehensive modeling of atomic-scale phononic metamaterial for the control of heat conduction by exploiting phonon interference antiresonances. Thermal phonons crossing crystal plane embedded with periodic defect-atom arrays experience strong reflection followed by total transmission, pointing out similarities of the phononic phenomena with their optical counterparts. Transmission antiresonances are not deteriorated by the aperiodicity in the defect-atom distribution and the anharmonicity of atom bonds. Such patterned atomic phononic mirrors with tunable frequency. The adjustment of the vibrational properties of the defect atoms and rational design of the defect-atom arrays can lead to a new approach to engineer thermal phonon spectrum,

thus offering possibilities of novel thermal effects and devices, such as high-efficiency atomic heat mirrors and insulators. At last, we would emphasize that strong optical reflection observed in stereometamaterials[9] can also be interpreted as an evidence for photon interference antiresonances in optically transparent plane, embedded with periodic plasmonic nanostructures.

* haoxue.han@ecp.fr

† sebastian.volz@ecp.fr

‡ yukosevich@gmail.com

- [1] U. Fano, Phys. Rev. **124**, 1866 (1961).
- [2] F. Hao, P. Nordlander, Y. Sonnefraud, P. V. Dorpe, and S. A. Maier, ACS nano **3**, 643 (2009).
- [3] Y. Sonnefraud *et al.*, ACS nano **4**, 1664 (2010).
- [4] M. Frimmer, T. Coenen, and A. F. Koenderink, Phys. Rev. Lett. **108**, 077404 (2012).
- [5] S. Fan and J.D. Joannopoulos, Phys. Rev. B **65**, 235112 (2002).
- [6] M. Rybin *et al.*, Phys. Rev. Lett. **103**, 023901 (2009).
- [7] V. A. Fedotov *et al.*, Phys. Rev. Lett. **99**, 147401 (2007).
- [8] S. Zhang *et al.*, Phys. Rev. Lett. **101**, 047401 (2008).
- [9] N. Liu, H. Liu, S. Zhu, and H. Giessen, Nature Photon. **3**, 157 (2009).
- [10] E. Altewischer, M. Van Exter, and J. Woerdman, Nature **418**, 304 (2002).
- [11] C. García-Meca *et al.*, Opt. Express **17**, 6026 (2009).
- [12] Yu. A. Kosevich, Prog. Surf. Sci. **55**, 1 (1997).
- [13] A. Fellay *et al.*, Phys. Rev. B **55**, 1707 (1997).
- [14] Yu. A. Kosevich, Physics-Uspekhi **51**, 848 (2008).
- [15] J. Zhu *et al.*, Nature Phys. **7**, 52 (2010).
- [16] Y. Xie, B.-I. Popa, L. Zigoneanu, and S. A. Cummer, Phys. Rev. Lett. **110**, 175501 (2013).
- [17] M. Eichenfield *et al.*, Nature **462**, 78 (2009).
- [18] J. Chan *et al.*, Nature **478**, 89 (2011).
- [19] S. Narayana and Y. Sato, Phys. Rev. Lett. **108**, 214303 (2012).
- [20] F. G. De Abajo, Rev. Mod. Phys. **79**, 1267 (2007).
- [21] Yu. A. Kosevich and E. S. Syrkina, Sov. Phys. Solid State **33**, 1156 (1991).
- [22] S. Plimpton, J. Comput. Phys. **117**, 1 (1995).
- [23] F. H. Stillinger and T. A. Weber, Phys. Rev. B **31**, 5262 (1985).
- [24] P. Schelling, S. Phillpot, and P. Keblinski, App. Phys. Lett. **80**, 2484 (2002).
- [25] H. Estrada *et al.*, Phys. Rev. Lett. **101**, 084302 (2008).
- [26] I. M. Khalatnikov, *An introduction to the theory of superfluidity* (Benjamin, New York, 1965).
- [27] Z. Liu *et al.*, Science **289**, 1734 (2000).
- [28] A. Degiron, H. Lezec, N. Yamamoto, and T. Ebbesen, Opt. Commun. **239**, 61 (2004).